Prediction of a Supersolid Phase in High-Pressure Deuterium

Chang Woo Myung[1], Barak Hirshberg[2,*] and Michele Parrinello[3,†]

[1]*Yusuf Hamied Department of Chemistry, University of Cambridge, Lenseld Road, Cambridge, CB2 1EW, United Kingdom*
[2]*School of Chemistry, Tel Aviv University, Tel Aviv 6997801, Israel*
[3]*Italian Institute of Technology, 16163 Genova, Italy*

Supersolid is a mysterious and puzzling state of matter whose possible existence has stirred a vigorous debate among physicists for over 60 years. Its elusive nature stems from the coexistence of two seemingly contradicting properties, long-range order and superfluidity. We report computational evidence of a supersolid phase of deuterium under high pressure ($p > 800$ GPa) and low temperature ($T < 1.0$ K). In our simulations, that are based on bosonic path integral molecular dynamics, we observe a highly concerted exchange of atoms while the system preserves its crystalline order. The exchange processes are favored by the soft core interactions between deuterium atoms that form a densely packed metallic solid. At the zero temperature limit, Bose-Einstein condensation is observed as the permutation probability of N deuterium atoms approaches $1/N$ with a finite superfluid fraction. Our study provides concrete evidence for the existence of a supersolid phase in high-pressure deuterium and could provide insights on the future investigation of supersolid phases in real materials.

Reports of an anomalous superfluid phase in solid ^{4}He [1] have spurred renewed interest in the study of this unusual state of matter, often referred to as a supersolid, in which long-range translational order and superfluidity are believed to coexist [1–14]. The very concept of a supersolid is puzzling since in a solid the nuclear density is localized around the equilibrium positions, while in a superfluid the nuclei wave functions are delocalized due to exchange [3,4,10–16].

Theoretical investigations [2–4,17] have preceded the first experimental reports of a ^{4}He supersolid [1]. Some of them argued that a supersolid could not exist [17] while others suggested that defects could favor its formation [2–4]. However, the experimental claim of [1] has been challenged [5–7], and it was pointed out that the defect formation energy in solid ^{4}He is too large to be invoked as a pathway to supersolidity [18]. Nevertheless, the search for a supersolid phase has not been abandoned and is still of great interest. Some encouragement in this direction comes from theoretical studies which indicate that a supersolid phase can be stabilized by suitable interparticle interactions [11–13,19], the dimensionality of the system [10,11,20] or optical coupling [14].

In this Letter, we report numerical evidence that deuterium at low temperature and high pressure can indeed become supersolid. There are various reasons why we pay attention to high pressure deuterium. First, the light mass of deuterium ($Z = 2$) leads to significant nuclear quantum effects (NQEs). Second, high level quantum mechanical calculations, such as density functional theory (DFT) and quantum Monte Carlo, predict that deuterium forms a metallic $I4_1/amd$ phase at $p > 500$ GPa [21,22]. Such a compressed environment promotes exchange interactions of deuterium atoms by bringing them closer. Third, it was argued that soft core interatomic potentials aid in favoring a supersolid phase [11]. In deuterium, the interactions between the nuclei in the metallic phase have screened Coulomb character which is softer than Lennard-Jones interactions. Last, the predicted phase transition pressure of the metallic $I4_1/amd$ phase ($p > 500$ GPa) appears to be within reach of experimental capabilities in the near future [23–26].

Simulating the quantum behavior of a supersolid phase of deuterium poses several challenges, such as (1) the accurate modeling of the interaction potential, (2) the inclusion of NQEs, and (3) the introduction of bosonic exchange symmetry. Here, we sketch the main points of our approach and refer the interested reader to a more detailed description of our methodology in Supplemental Material [27]. Following the approach pioneered by Behler and Parrinello [47], the interaction potential is described by a feed forward neural network potential, that is trained on a large number of DFT calculations. We chose the vdW-DF2 functional based on the generalized gradient approximation with nonlocal correlations [48] (Supplemental Material [27], Sec. I).

NQEs are described by using a discretized version of Feynman's path integral expression for the quantum partition function that is sampled in molecular dynamics simulations (PIMD) [49] by exploiting its well-known isomorphism with a system of classical ring polymers [50]. Exchange symmetry is dealt with using the bosonic
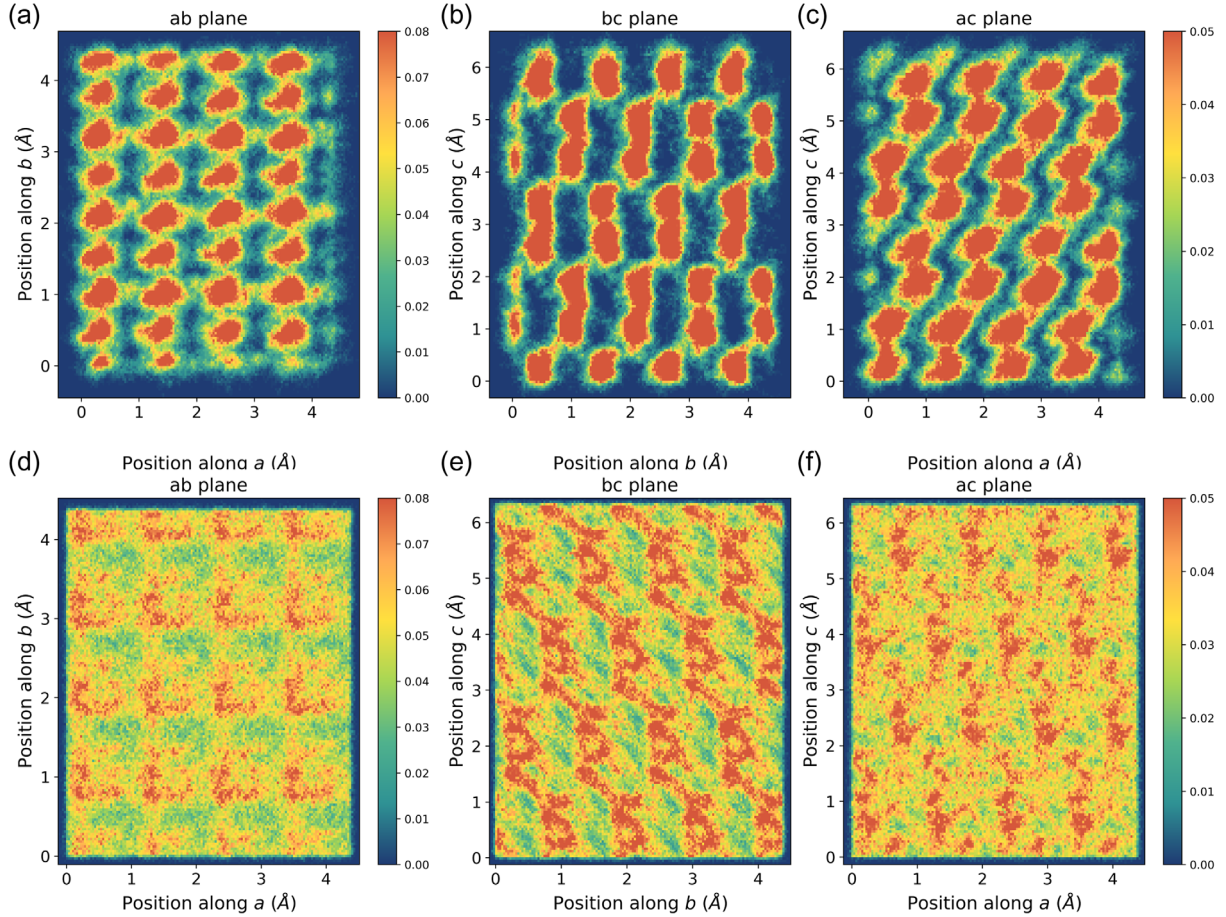
FIG. 1. Atomic density of high-pressure deuterium solid with exchange. Two-dimensional (2D) cross sections of the atomic density $n(r)$ of high-pressure deuterium in path integral molecular dynamics (PIMD) (a)–(c) and bosonic path integral molecular dynamics (PIMDB) (d)–(f) simulations at $p = 800$ GPa and $T = 0.5$ K. While the ring polymers of PIMD simulation are always closed form (a)–(c), the PIMDB simulations allow deuterium atoms to exchange (d)–(f).

version of path integral molecular dynamics (PIMDB) of Hirshberg *et al.* [51,52]. This is done by evaluating the PIMD potential for N bosons recursively,

$$e^{-\beta V_B^{(N)}} = \frac{1}{N} \sum_{k=1}^{N} e^{-\beta (E_N^{(k)} + V_B^{(N-k)})}, \qquad (1)$$

where β is the inverse temperature, $V_B^{(N-k)}$ is the PIMD potential for $N - k$ bosons, and $E_N^{(k)}$ is the spring energy of a ring polymer constructed by connecting all of the beads of k particles sequentially [51]. The method provides the correct bosonic thermal expectation values while avoiding the need to enumerate all $N!$ permutations of identical particles. This reduces the computational scaling of PIMDB simulations from factorial to cubic, allowing large bosonic systems to be simulated using PIMD [51]. We have explicitly checked that this method [52] gives results in full agreement with those obtained using the path integral Monte Carlo (PIMC) method pioneered by Ceperley [16]. Our evaluation of superfluid fractions of liquid ^{4}He

[16] and hcp solid ^{4}He [18] concurred with the previous PIMC results (Supplemental Material [27], Figs. 12 and 13). For deuterium, we note that the current implementation only considers the spatial permutations of atoms with the same spin-projection (Supplemental Material [27], Sec. III). Thus, our estimation is relevant to a spin-polarized system and might lead to a slight overestimation of the superfluid transition temperature.

To perform simulations at constant pressure, we implemented the isothermal-isobaric (NPT) PIMD algorithm and adapted it to use the correct pressure estimator for bosons (Supplemental Material [27], Sec. II). Although we have studied the system at different thermodynamic conditions, we report the results obtained at $p = 800$ GPa in a range of low temperatures from $T = 0.1$ K to $T = 1.2$ K in the main text. Additional thermodynamic conditions are found in Supplemental Material [27]. We find that converged results can be obtained if we discretize the Feynman path using $P = 256$ beads (Supplemental Material [27], Fig. 7).

In order to bring out the role of NQEs and exchange symmetry, we performed simulations of solid deuterium
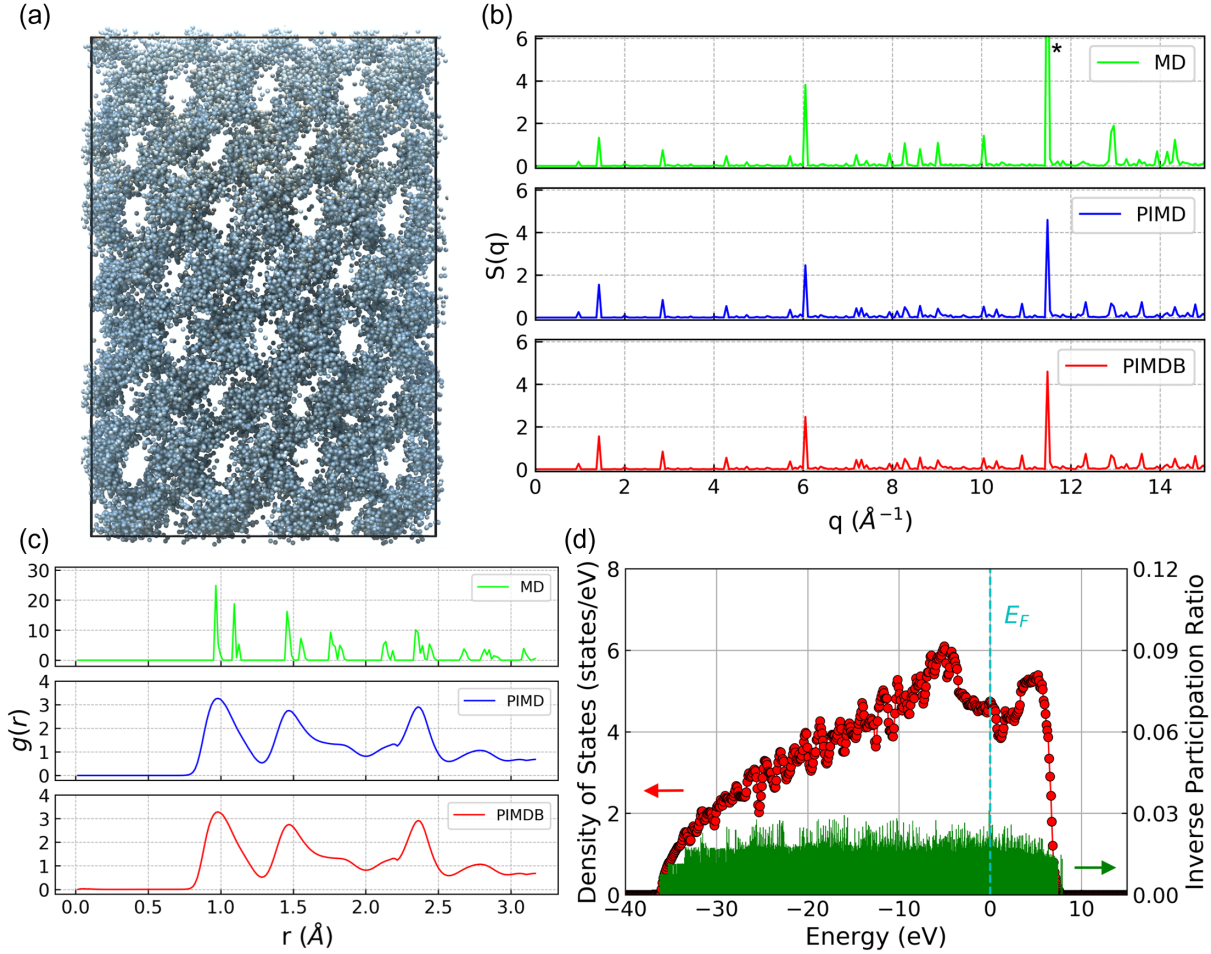
FIG. 2. Exchange effect on the geometry and electronic properties of high-pressure deuterium. (a) A snapshot taken from the $(N \times P)$ trajectory of PIMDB simulations at $T = 0.5$ K and $p = 800$ GPa. Each blue sphere represents a one bead of a ring polymer (in total $P = 256$ beads and $N = 128$). (b) Structure factors $S(q)$ of high-pressure deuterium from the MD (green line), PIMD (blue line), and PIMDB (red line) simulations. The amplitude of omitted $S(q)$ peak (*) of the MD simulation (green) is 14.9. (c) Radial distribution functions $g(r)$ of high-pressure deuterium from the MD (green line), PIMD (blue line), and PIMDB (red line) simulations. (d) The density of states (red points) and inverse participation ratio (green bars) of a supersolid phase. The Fermi level (E_F) is set to zero (cyan dashed line).

using three different methods, treating deuterium as (1) a classical particle (MD), (2) a distinguishable quantum particle (PIMD), and (3) an indistinguishable boson (PIMDB) (Figs. 1 and 2). The average density $n(r)$ is greatly affected by exchange processes (Fig. 1).

Even for distinguishable deuterium the NQEs make the atomic density distribution of neighboring atoms overlap [Figs. 1(a)–1(c)]. This overlap suggests the possible role of exchange processes. Indeed, as the exchange of deuterium atoms is allowed via PIMDB simulation, it is difficult to spot the precise equilibrium positions of deuterium $I4_1/amd$ phase due to active exchange [Figs. 1(d)–1(f)]. This implicates that the connected ring polymers of deuterium atoms emerge at low temperatures [Figs. 1(d)–1(f)]. At first sight [Fig. 2(a)], it would appear that the $n(r)$ would correspond to that of a glassy system, however, our analysis shows that the $I4_1/amd$ symmetry is hidden but not lost [Figs. 2(b) and 2(c)]. To show it, we evaluated the structure factor,

$$S(q) = \frac{1}{PN} \sum_{\tau=1}^{P} \sum_{j,k=1}^{N} e^{-i\mathbf{q}(\mathbf{R}_j^{(\tau)} - \mathbf{R}_k^{(\tau)})}, \quad (2)$$

where $P, N, \mathbf{R}_j^{(\tau)}$ are the number of beads, the number of particles, and position of atom j at τ imaginary time, respectively. Bragg peaks can be clearly seen with and without exchange at the same positions in reciprocal space [Fig. 2(b) and Supplemental Material [27], Fig. 8]. Thus, the result indicates that this peculiar exchange of deuterium does not break the solid long-range order. Also, the pair correlation of the solid phase is preserved under exchange interactions as evidenced by the radial distribution function $g(r)$ of MD, PIMD, and PIMDB simulations [Fig. 2(c)]. Even in the active exchange regime, the system still remains metallic as the solid phase. This can be understood given that this anomalous deuterium phase preserves the solid long-range order. Thus, the density of states [Fig. 2(d)] is similar
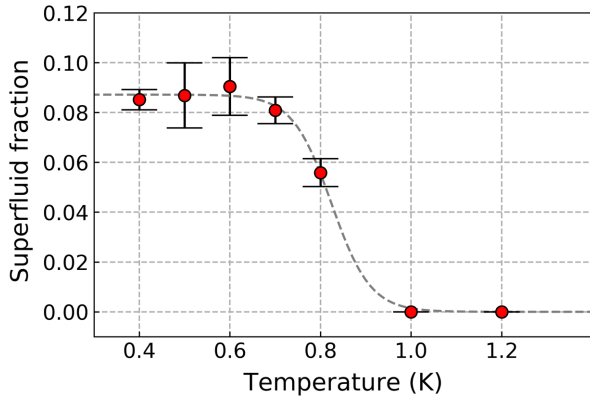
FIG. 3.   The superfluid fraction of high-pressure deuterium. The superfluid fraction (red points with error bar) at $p = 800$ GPa as the function of temperature with a guiding line (dotted gray line).

to that of the solid [Supplemental Material [27], Fig. 2(b)]. The presence of disorder in a supersolid phase might introduce the localization of electronic states [53]. However, our analysis based on the inverse participation ratio shows that the electronic states of supersolid phase are delocalized [Fig. 2(d) and Supplemental Material [27], Sec. III].

The fact that one can reconcile long-range order and a very active exchange regime remains puzzling also in the Feynman isomorphism. In order to get insight into how this is possible, we look at the bead's spatial arrangement as it evolves during the simulation where all permutations contribute to the forces on atoms at each time step [51]. This can be measured by a structure factor of the beads system considered as a set of independent particles $S_{\text{rel}}(q) = (1/PN) \sum_{\tau,\tau'=1}^{P} \sum_{j,k=1}^{N} e^{-iq(\mathbf{R}_j^{(\tau)} - \mathbf{R}_k^{(\tau')})}$. While the beads distribution changes dynamically from one time step to another, the overall long-range order of $(P \times N)$ configuration is still preserved (Supplemental Material [27], Fig. 9). This points to a highly coherent exchange mechanism.

An elegant way of measuring whether a system is superfluid is to compute its winding number [54]. This quantity reflects the number of paths that, due to exchange, are so long that they wrap around the periodic boundary conditions [54]. In our approach, in which all permutations are sampled at every time step, standard methods to evaluate it cannot be applied. Therefore, we have developed an approximate but highly accurate approach to measure the winding number in PIMDB simulations (Supplemental Material, Sec. III and Supplemental Material [27], Fig. 11). The result obtained is presented in Fig. 3. It shows that at $T < 1.0$ K a superfluid condensate is formed. The analysis of the probability of observing longer rings also confirms this picture (Supplemental Material [27], Fig. 12). Our calculation shows that for high pressure deuterium a defect-free pathway to supersolidty is possible.

Experiments on such thermodynamic conditions will be feasible in the near future given the rapid advancement of diamond anvil cell techniques at cryogenic temperature [23–25], and verifying this prediction in experiments will be a fascinating challenge to undertake.

All the implementations of the isotropic and full-cell NPT simulations of PIMDB are freely available in the author's GitHub repository [55]. All the necessary input files of this computational study are also available in the author's Github repository [56].

[*]hirshb@tauex.tau.ac.il
[†]michele.parrinello@iit.it

[1] E. Kim and M. H. Chan, Nature (London) **427**, 225 (2004).
[2] D. Thouless, Ann. Phys. (N.Y.) **52**, 403 (1969).
[3] A. F. Andreev and I. M. Lifshitz, Sov. Phys. JETP **29**, 1107 (1969).
[4] G. V. Chester, Phys. Rev. A **2**, 256 (1970).
[5] J. Day and J. Beamish, Nature (London) **450**, 853 (2007).
[6] B. Hunt, E. Pratt, V. Gadagkar, M. Yamashita, A. V. Balatsky, and J. C. Davis, Science **324**, 632 (2009).
[7] T. Kreibich, R. van Leeuwen, and E. K. U. Gross, Phys. Rev. A **78**, 022501 (2008).
[8] M. Boninsegni and N. V. Prokof'ev, Rev. Mod. Phys. **84**, 759 (2012).
[9] V. I. Yukalov, Physics **2**, 49 (2020).
[10] F. Mezzacapo and M. Boninsegni, Phys. Rev. Lett. **97**, 045301 (2006).
[11] F. Cinti, P. Jain, M. Boninsegni, A. Micheli, P. Zoller, and G. Pupillo, Phys. Rev. Lett. **105**, 135301 (2010).
[12] L. Tanzi, S. M. Roccuzzo, E. Lucioni, F. Famà, A. Fioretti, C. Gabbanini, G. Modugno, A. Recati, and S. Stringari, Nature (London) **574**, 382 (2019).
[13] J. R. Li, J. Lee, W. Huang, S. Burchesky, B. Shteynas, F. Ç. Topi, A. O. Jamison, and W. Ketterle, Nature (London) **543**, 91 (2017).
[14] J. Léonard, A. Morales, P. Zupancic, T. Esslinger, and T. Donner, Nature (London) **543**, 87 (2017).
[15] P. Sindzingre, D. M. Ceperley, and M. L. Klein, Phys. Rev. Lett. **67**, 1871 (1991).
[16] D. M. Ceperley, Rev. Mod. Phys. **67**, 279 (1995).

[17] L. Penrose and O. Onsager, Phys. Rev. **104,** 576 (1956).

[18] D. M. Ceperley and B. Bernu, Phys. Rev. Lett. **93,** 155303 (2004).

[19] Y. Kora and M. Boninsegni, J. Low Temp. Phys. **197,** 337 (2019).

[20] F. Mezzacapo and M. Boninsegni, J. Phys. Chem. A **115,** 6831 (2011).

[21] J. M. McMahon and D. M. Ceperley, Phys. Rev. Lett. **106,** 165302 (2011).

[22] S. Azadi, B. Monserrat, W. M. C. Foulkes, and R. J. Needs, Phys. Rev. Lett. **112,** 165501 (2014).

[23] P. Dalladay-Simpson, R. T. Howie, and E. Gregoryanz, Nature (London) **529,** 63 (2016).

[24] C. Ji, B. Li, W. Liu, J. S. Smith, A. Majumdar, W. Luo, R. Ahuja, J. Shu, J. Wang, S. Sinogeikin, Y. Meng, V. B. Prakapenka, E. Greenberg, R. Xu, X. Huang, W. Yang, G. Shen, W. L. Mao, and H. K. Mao, Nature (London) **573,** 558 (2019).

[25] R. P. Dias and I. F. Silvera, Science **355,** 715 (2017).

[26] P. Loubeyre, F. Occelli, and P. Dumas, Nature (London) **577,** 631 (2020).

[27] See Supplemental Material at http://link.aps.org/supplemental/10.1103/PhysRevLett.128.045301 about the method implementation, simulation details, and additional results, which includes Refs. [18,28–46].

[28] X.-Z. Li, B. Walker, M. I. J. Probert, C. J. Pickard, R. J. Needs, and A. Michaelides, J. Phys. Condens. Matter **25,** 085402 (2013).

[29] T.-T. Cui, J.-C. Li, W. Gao, J. Hermann, A. Tkatchenko, and Q. Jiang, J. Phys. Chem. Lett. **11,** 1521 (2020).

[30] K. Berland, V. R. Cooper, K. Lee, E. Schröder, T. Thonhauser, P. Hyldgaard, and B. I. Lundqvist, Rep. Prog. Phys. **78,** 066501 (2015).

[31] R. Sabatini, E. Küçükbenli, B. Kolb, T. Thonhauser, and S. De Gironcoli, J. Phys. Condens. Matter **24,** 424209 (2012).

[32] P. Giannozzi *et al.*, J. Phys. Condens. Matter **29,** 465901 (2017).

[33] C. J. Pickard and R. J. Needs, Nat. Phys. **3,** 473 (2007).

[34] P. Cudazzo, G. Profeta, A. Sanna, A. Floris, A. Continenza, S. Massidda, and E. K. U. Gross, Phys. Rev. Lett. **100,** 257001 (2008).

[35] H. Wang, L. Zhang, J. Han, and W. E, Comput. Phys. Commun. **228,** 178 (2018).

[36] L. Zhang, J. Han, H. Wang, W. A. Saidi, R. Car, and E. Weinan, Adv. Neural Inf. Process. Syst. **2018,** 4436 (2018), https://arxiv.org/abs/1805.09003.

[37] F. Pederiva, G. V. Chester, S. Fantoni, and L. Reatto, Phys. Rev. B **56,** 5909 (1997).

[38] G. J. Martyna, A. Hughes, and M. E. Tuckerman, J. Chem. Phys. **110,** 3275 (1999).

[39] G. J. Martyna, M. E. Tuckerman, D. J. Tobias, and M. L. Klein, Mol. Phys. **87,** 1117 (1996).

[40] A. P. Lyubartsev and P. N. Vorontsov-Velyaminov, Phys. Rev. A **48,** 4075 (1993).

[41] D. M. Ceperley, J. Stat. Phys. **63,** 1237 (1991).

[42] C. Colliex, J. M. Cowley, S. L. Dudarev, M. Fink, J. Gjønnes, R. Hilderbrandt, A. Howie, D. F. Lynch, L. M. Peng, G. Ren, A. W. Ross, V. H. Smith, J. C. H. Spence, J. W. Steeds, J. Wang, M. J. Whelan, and B. B. Zvyagin, *International Tables for Crystallography Volume c: Mathematical, Physical and Chemical Tables* (Springer Netherlands, Dordrecht, 2004), pp. 259–429.

[43] L.-M. Peng, G. Ren, S. L. Dudarev, and M. J. Whelan, Acta Crystallogr. Sect. A **52,** 257 (1996).

[44] R. A. Aziz and H. H. Chen, J. Chem. Phys. **67,** 5719 (1977).

[45] W. Krauth, Phys. Rev. Lett. **77,** 3695 (1996).

[46] J. Chen, X. Li, Q. Zhang, M. I. Probert, C. J. Pickard, R. J. Needs, A. Michaelides, and E. Wang, Nat. Commun. **4,** 2064 (2013).

[47] J. Behler and M. Parrinello, Phys. Rev. Lett. **98,** 146401 (2007).

[48] T. Thonhauser, V. R. Cooper, S. Li, A. Puzder, P. Hyldgaard, and D. C. Langreth, Phys. Rev. B **76,** 125112 (2007).

[49] M. Parrinello and A. Rahman, J. Chem. Phys. **80,** 860 (1984).

[50] D. Chandler and P. G. Wolynes, J. Chem. Phys. **74,** 4078 (1981).

[51] B. Hirshberg, V. Rizzi, and M. Parrinello, Proc. Natl. Acad. Sci. U.S.A. **116,** 21445 (2019).

[52] B. Hirshberg, M. Invernizzi, and M. Parrinello, J. Chem. Phys. **152,** 171102 (2020).

[53] P. W. Anderson, Phys. Rev. **109,** 1492 (1958).

[54] E. L. Pollock and D. M. Ceperley, Phys. Rev. B **36,** 8343 (1987).

[55] https://github.com/changwmyung/lammps/tree/NPT_PIMD.

[56] The supporting data for this Letter are freely available in the author's Github repository, https://github.com/changwmyung/deuterium_supersolid.